J6J.1 PEEPING THROUGH THE KEYHOLE AT THE MESOSCALE VARIABILITY OF HUMIDITY: SOME IHOP_2002 OBSERVATIONS AND FUTURE CHALLENGES OF RADAR REFRACTIVITY MAPPING

Frédéric Fabry
McGill University, Montreal, Quebec, Canada

1. CONVECTION INITIATION AND HUMIDITY

Despite the continuous improvement in observation and modeling tools, warm-season forecasting of precipitation remains a considerable challenge. Lower forecasting skills in summer are associated with the fact that rainfall in that season has a more convective nature that greatly depends on the inadequately observed mesoscale variability of dynamical and thermodynamic fields. Water vapor is one of the least well measured of these variables. As a result, "on the storm scale, prediction of convective precipitation is limited by uncertainty in the distribution of water vapor in the atmosphere and the amount of water in the soil" (National Research Council 1998).

Because our tools for observing kinematics at the mesoscale (such as radars) have been considerably better than those used to observe thermodynamic parameters (mainly in-situ sensors), detailed field studies of convection initiation (CI) have focused on dynamics issues such as the importance of convergence boundaries and small-scale circulations along them. The International H_2O Project was put together to address the issues associated with the time varying, 3-D distribution of water vapor and its impact on the understanding and prediction of warm season precipitation events (Weckwerth et al. 2004). Even with the array of instruments deployed, moisture (and temperature) remained considerably less well characterized than winds or even precipitation.

2. RADAR MEASUREMENTS OF REFRACTIVITY

One of the instruments deployed during IHOP_2002 was the National Center for Atmospheric Research S-Pol radar. In addition to reflectivity, Doppler velocity, and many dual-polarization parameters, S-Pol measured the near-surface refractivity of air, a quantity closely related to surface moisture (Fabry et al. 1997; Fabry 2004; Weckwerth et al. 2005). Refractivity measurements by radar offer us our first glimpse at the 2-D structure of near-surface moisture at the mesoscale. While most moisture measurements until now had been limited to point values and vertical profiles, refractivity measurements allow us to observe the time evolution of moisture field in the same way that radar reflectivity made possible the study of the mesoscale structure of precipitation.

Corresponding author address: Frédéric Fabry, McGill Univ., Dept. of Atmospheric and Oceanic Sciences, Montreal, QC, H3A 2K6 Canada; e-mail: frederic.fabry@mcgill.ca

But that glimpse is limited. While radars can measure reflectivity up to ranges exceeding 200 km, the average range up to which one can observe refractivity fields is generally limited to 40 km (Fig. 1). The experience is a bit analogous to that of peeping through a keyhole: the information you gather is of great value because it is not easily obtainable otherwise; you feel privileged and are eager to watch previously unobserved events, finally understand more about their nature and the process; and you keep cursing at the limited field of view, always wishing you could see more.

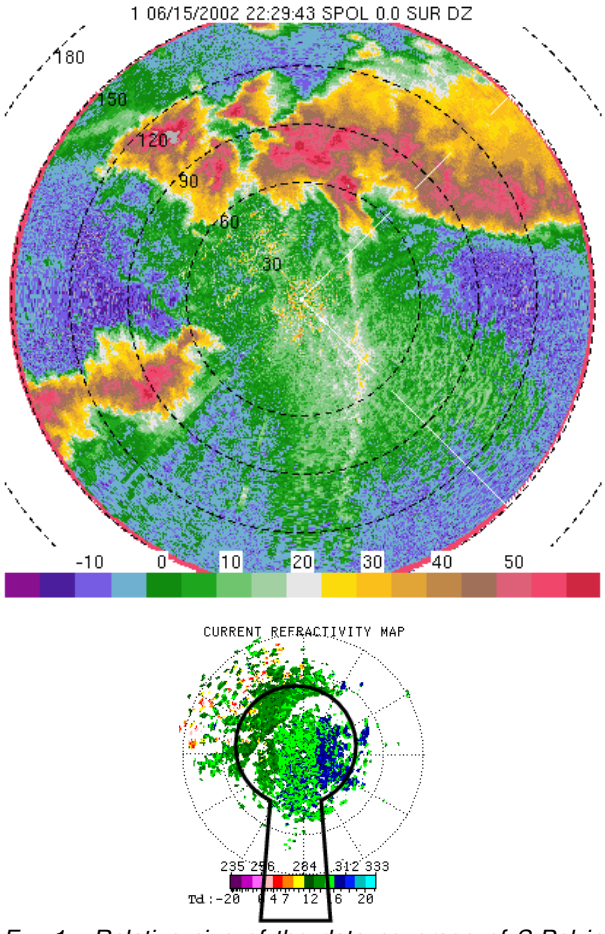

FIG. 1: Relative size of the data coverage of S-Pol in reflectivity (above) and refractivity (below) during IHOP. The overlay on the refractivity map is a keyhole outline.

Radar measures refractivity between a ground-based radar generally perched a few tens of meters above the surface, and ground targets that can be at the surface or extending at most up to a few hundreds of

meters high (Fig. 2). Refractivity measurements by radar are hence representative of atmospheric conditions just above the surface. This makes these measurements particularly interesting for the study of boundary-layer processes, surface boundaries such as fronts, surface-based convection initiation, and storm outflows.

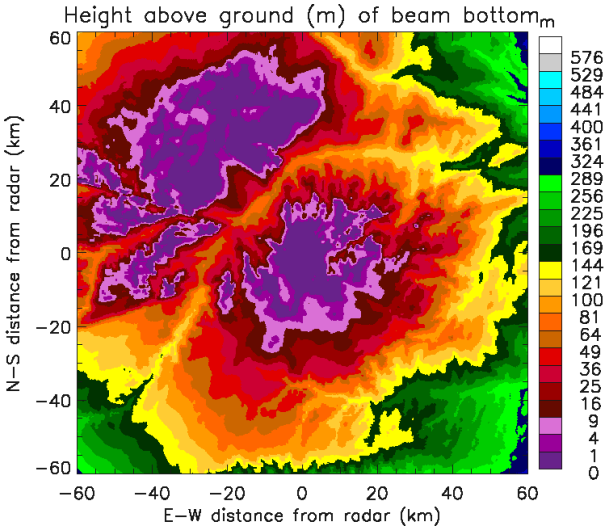

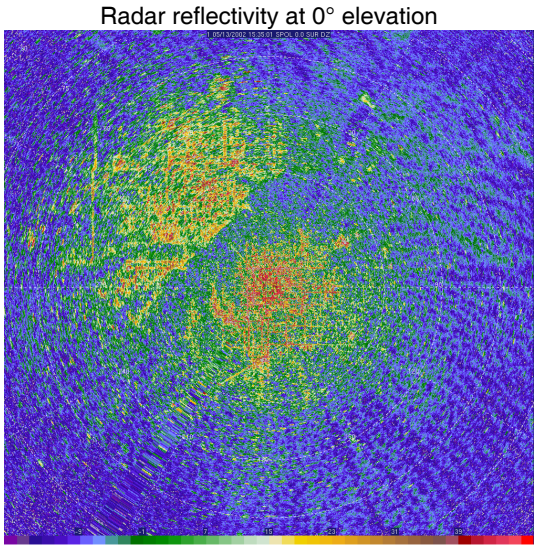

FIG. 2: Top: Predicted height of the bottom part of the beam still unblocked by topography under normal propagation conditions (program courtesy of ShinJu Park). A height of 0 means that a portion of the beam is intercepting the ground; ground targets will be observed in non-zero areas only if targets extend vertically above the stated height. Below: Reflectivity map at low-elevation angles at the same scale. Echoes more intense than sub-zero dBZ insects (from greens to reds) are caused by ground targets; many of them are intercepted wherever the bottom part of the beam is below 15 m, but not beyond. Radar measurements of refractivity are hence generally made below 15 m AGL.

3. SOME IHOP_2002 EXAMPLES

3.1 Boundary-layer moisture variability

Moisture variability is observed at all scales (Fig. 3), and has impacts on clouds and stability fields (Fig. 4).

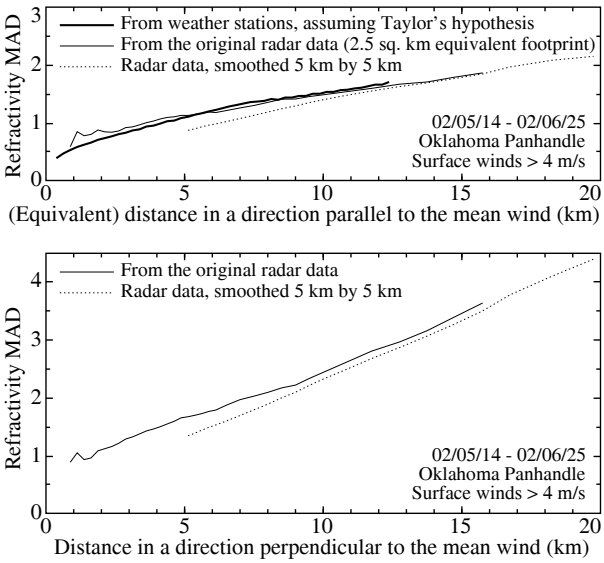

FIG. 3: Mean absolute differences (MAD) in refractivity between neighboring points as a function of their distance in a direction parallel (top) or perpendicular (bottom) to the mean wind for all time periods during IHOP_2002 where the wind was stronger than 4 m s^{-1}. See Fabry (2005) for details.

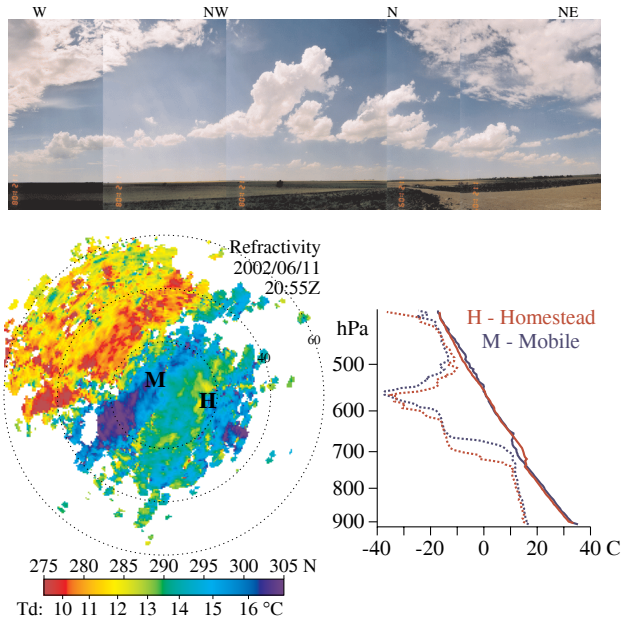

FIG. 4: Top: Cloud field as observed from the S-Pol radar. The line of cumulus clouds is associated with a convergence line and a moisture tongue observed on refractivity (bottom left) and, to a smaller extent, on radiosonde measurements from two sites (bottom right).

Refractivity is a good tracer of the thermodynamic properties of air. Processes that affect these properties or that transport air can hence be spotted. For example, convergence lines that strengthen humidity and temperature gradients often appear first on refractivity before the associated updrafts have the time to lift enough insects to form a reflectivity fine line (Fig. 5). Sometimes, the effects of smaller-scale phenomena such as boundary layer rolls or misocyclones (Fig. 6) can also be detected.

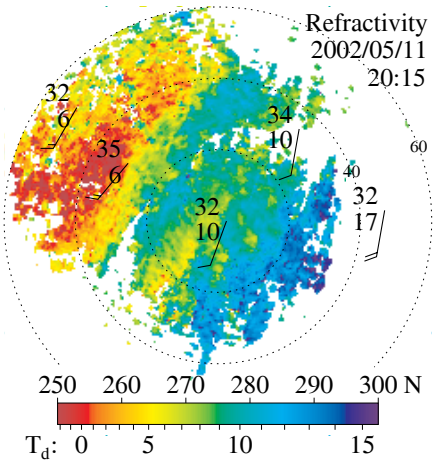

FIG. 5, right: Example of a refractivity field on May 11 at a time when the dry line has not yet collapsed into a single line visible on radar reflectivity. The refractivity scale also shows the corresponding dew point temperatures given the average pressure and temperature conditions at 20:15 UTC.

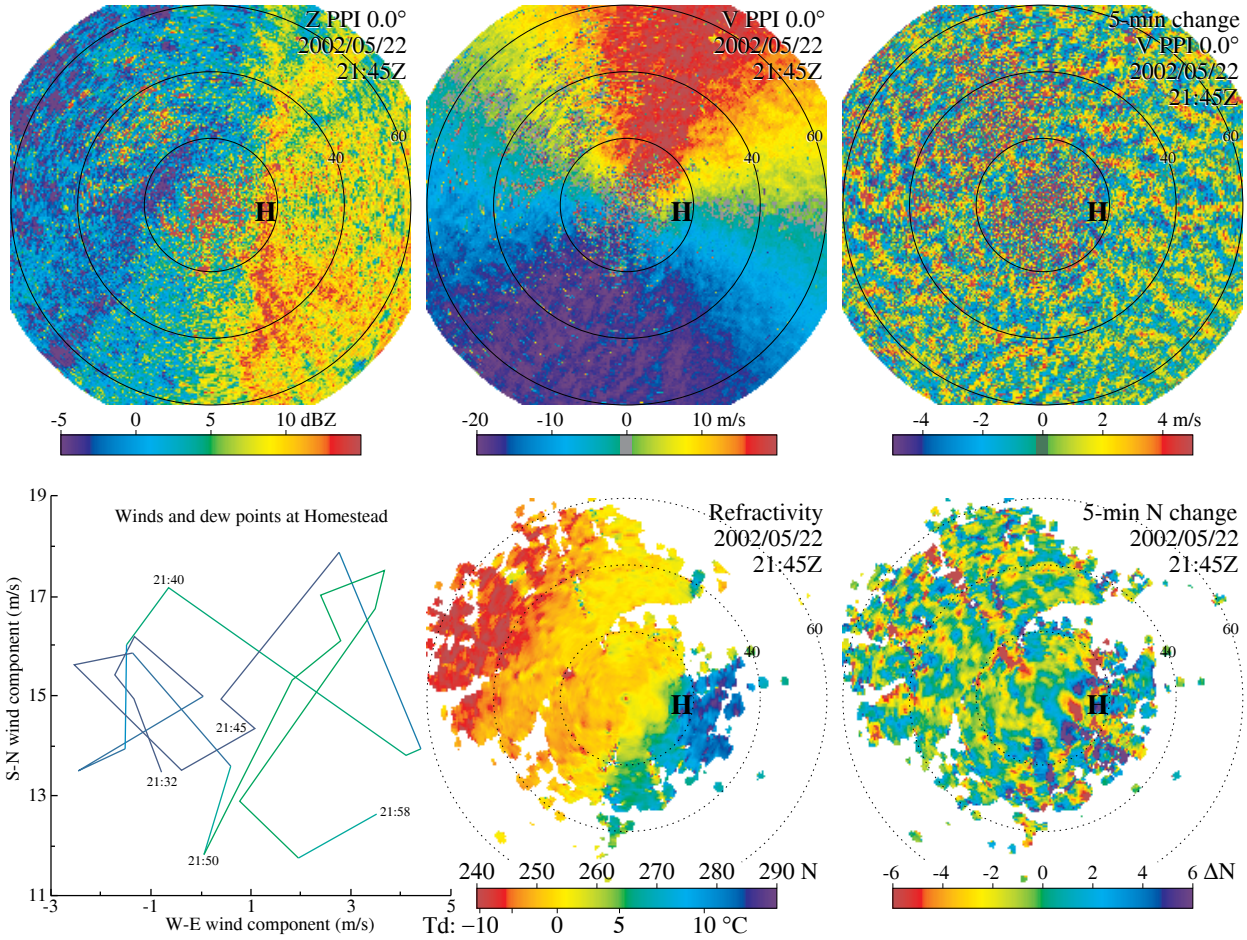

FIG. 6. Detailed snapshot of the May 22 multiple dry lines. On reflectivity (top left) and Doppler velocity (top middle), one can observe a convergence line standing over the Homestead site (H). But on refractivity (bottom middle), we can observe several moisture boundaries: one associated with the observed fine line passing immediately east of Homestead; one oriented SSW-NNE and passing immediately west of Homestead; and a broader line oriented SSW-NNE 40 km west of the radar. The second boundary will grow a reflectivity fine line in the following hour. The refractivity and the refractivity change (bottom right) images also show that these boundaries are wiggly; this is probably due to the presence of misocyclones on the boundaries, which would explain why the Doppler field changes in time more in these regions than elsewhere (top right). Although there appears to be a fair anti-correlation between the refractivity change and the Doppler change fields along the boundaries, surface observations of winds and dew points (bottom left) do not paint a clear picture. For more on this case: Weckwerth et al. (2004); Demoz et al. (2005).

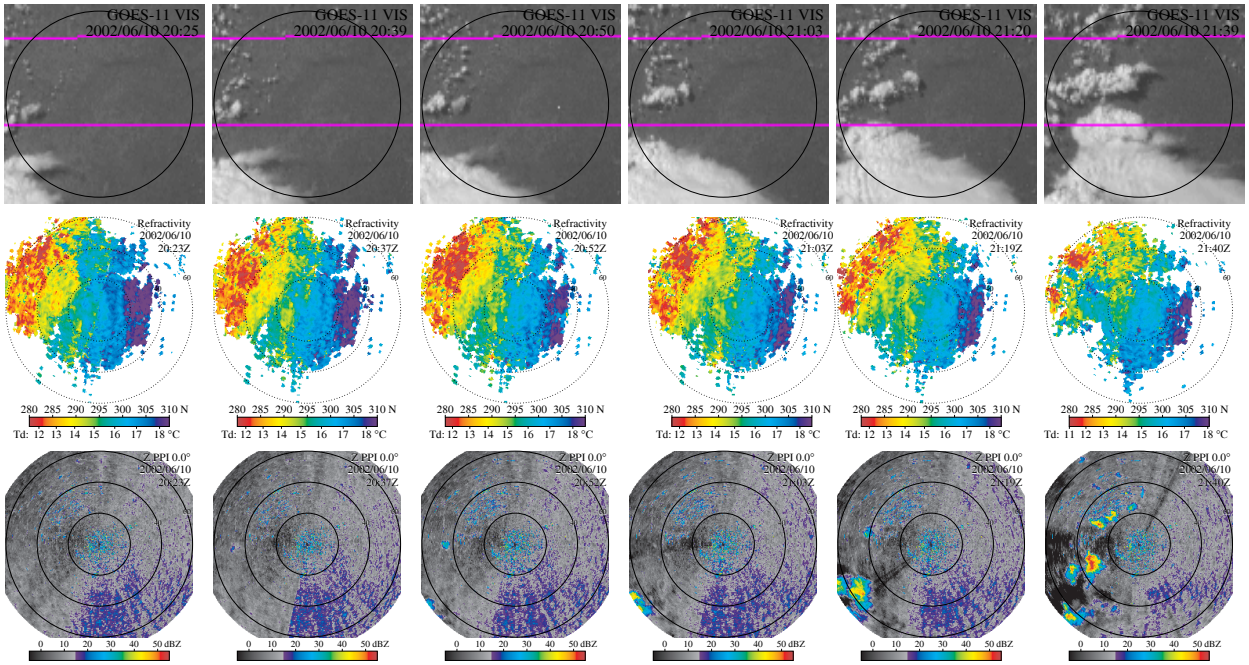

FIG. 7. Time sequence of visible imagery (top), refractivity (middle), and reflectivity factor (bottom) of the initiation of convection within refractivity coverage of S-Pol on 10 June 2002. To increase data quality especially at far ranges, the refractivity images were obtained by averaging three successive images displaced to account for the wind.

3.2 Convection initiation example

Most of the convection initiation that occurred very close to S-Pol during IHOP_2002 was at night. Since these events are not surface-forced, they are not often associated with interesting surface refractivity fields. Three daytime cases occurred and are briefly discussed in Fabry (2005) (May 11) and Weckwerth et al. (2005) (June 10 and 12). Here, I will focus on the 10 June event (Fig. 7).

On June 10, several cumuli were developing west of a moisture contrast line observed 40 km west of S-Pol. These cumuli were advected eastward, where they crossed the moisture contrast line and underwent further development. For example, the cumuli to the west and north-west of S-Pol went from being non-precipitating to reaching reflectivities of 50 dBZ. Note that here again, no reflectivity signature can be observed associated with the lines of humidity contrast.

At this stage, we have not been able to find clear predictors of convection initiation on the refractivity fields. One of the possible reasons is that moisture variability is only one of several parameters that affect the likelihood of initiation. If we concentrate on dynamic and thermodynamic variability without focusing on their causes, we find via a simulation using aircraft observations that temperature is the most important parameter affecting CIN at large scales, while updraft strength is the most important parameter at small scales (Fig. 8; Fabry 2005). Moisture seems to play second fiddle at both larger and smaller scales. One might conclude from this exercise that measurements of refractivity would then offer little information on initiation because of the apparent limited impact of moisture

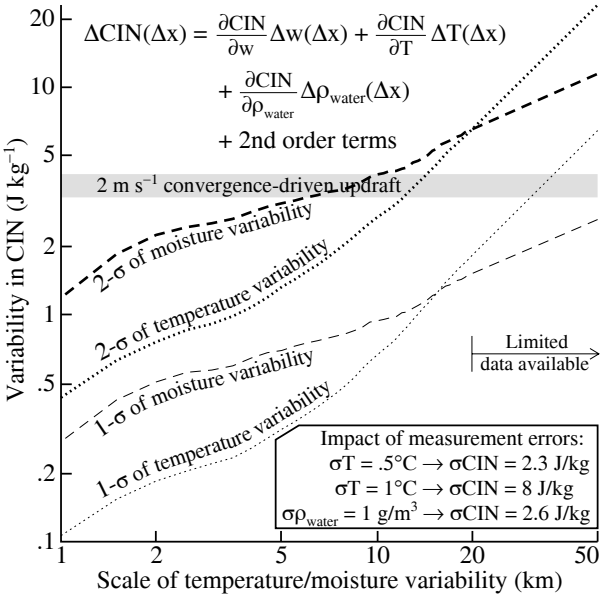

FIG. 8. Effect of the observed variability in temperature (dotted line) and moisture (dashed line) on convective inhibition (CIN) in the upper BL as a function of the scale over which that variability is observed. The contributions to CIN variability of the one- and two-standard deviations of the distribution of temperature and moisture observed at a given scale are contrasted with the effect of a 2 m s^{-1} convergence-driven updraft using the formula of Crook and Klemp (2000).

variability on CI: the key to CI prediction is and remains the detection of convergence zones. Such a conclusion would neglect the fact that refractivity measurements are extremely valuable to detect these convergence regions: in many instances, convergence lines were observed on refractivity sometimes several hours before a reflectivity fine line could be identified. An ironic conclusion of this work is that although the interest on refractivity has been centered on its ability to estimate moisture, high resolution refractivity measurements may end up being crucial for CI prediction solely to resolve the otherwise hidden small-scale dynamics!

3.3 Storm outflows

The phenomenon that generates the most complex and contrasted refractivity fields is daytime storm outflows. Outflows can travel great distances; hence many outflows of different "age" were observed in IHOP.

If we continue looking at the 10 June case, we will see two significant outflows passing over the domain (Fig. 9). The first was generated by storms outside the domain (approximately 90 km to the SW) and passed over S-Pol at 21:50Z. The second formed from the storm immediately south of S-Pol around 22:30 and reached the radar at 22:50Z. In both cases, the outflow, which had initially a refractivity comparable to that of boundary layer air, quickly became drier with time. This can be understood if one visualizes the vertical profile of moisture in a storm: the air that first comes out of the thunderstorm downdraft is boundary layer air, gradually followed by air from increasingly high levels in the free atmosphere. In the outflow, one must hence expect to see air of uniform moisture until all air of boundary layer origin has been pushed out; then, progressively drier air should come out, to some extent mimicking the dew point temperature profile of the atmosphere where the downdraft formed (Fig. 10).

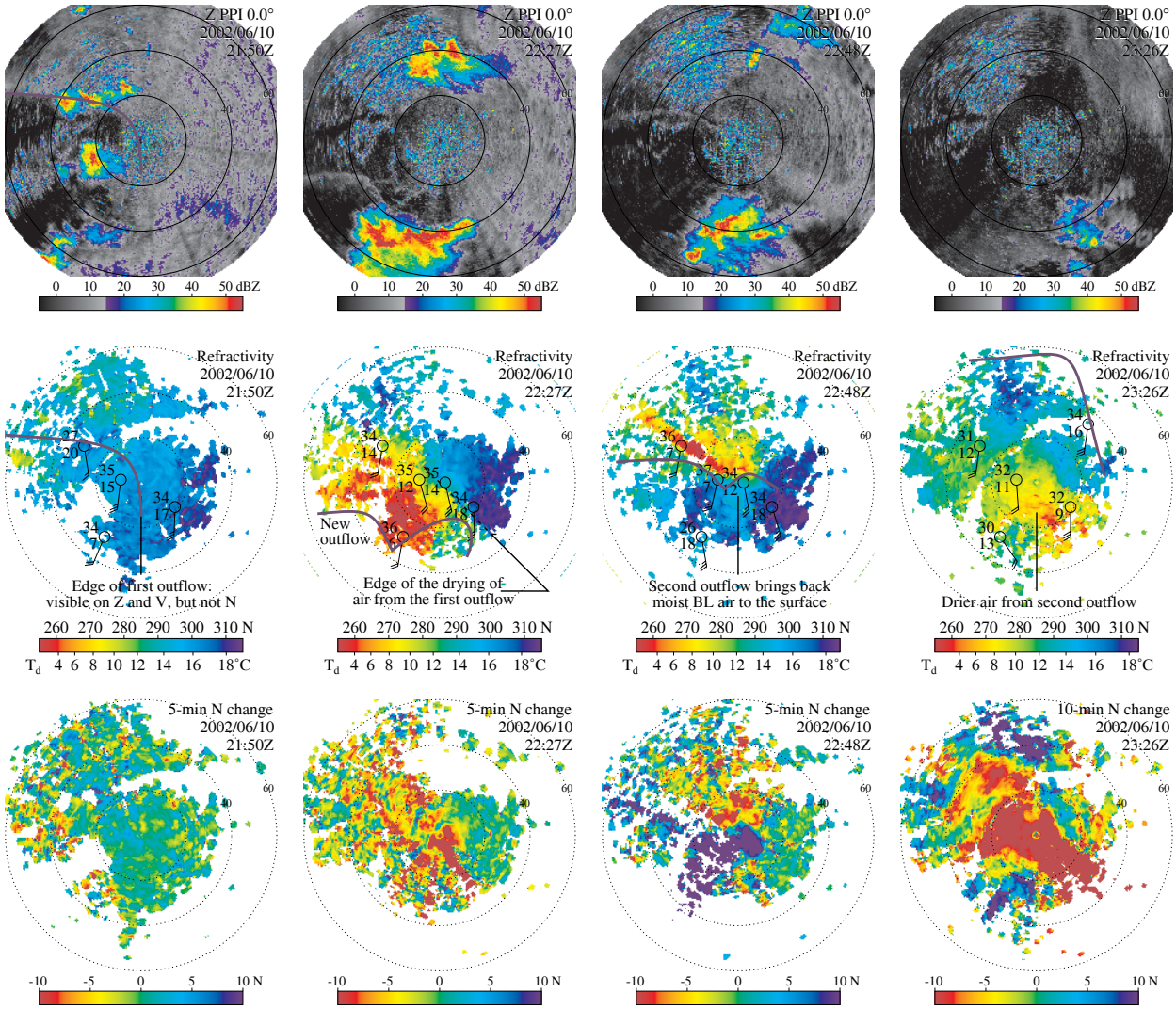

FIG. 9. Time sequence of reflectivity (top), refractivity (middle), and refractivity change (bottom) during the passage of two storm outflows on 10 June 2002. For both outflows, the air becomes progressively drier in time.

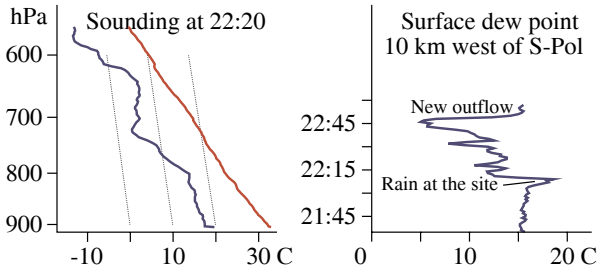

FIG. 10. Left: Temperature and dew point sounding from Homestead (16 km east of S-Pol) at 22:20. Dotted lines represent lines of constant mixing ratios. Right: Dew point temperature measured by the Playhouse station 10 km west of S-Pol from the time of passage of the first outflow boundary (21:35) and until after the passage of the second outflow boundary. Except for the effect of a rain shower at the Playhouse site after 22:00, one can see that the dew point time series mimics the vertical profile of mixing ratios measured by the sounding.

4. (FUTURE) TECHNICAL CHALLENGES

The technique used until now for extracting refractivity fields from the phase of ground targets (Fabry 2004) works well at long wavelengths and over very flat terrain, preferably in the absence of very strong gradients in *N*. There is however growing interest to apply the technique 1) on magnetron-based systems, 2) on systems with shorter wavelengths, and 3) on many types of sites, including those with a complex topography. The first issue is essentially a "simple" hardware one: the technique *can* easily be adapted to systems with transmitters whose frequency change with time (such as magnetrons), provided that the changing frequency is accurately measured. The two others will require rethinking the technique with three dimensions in mind instead of two, and solve two problems: reduce the noisiness of the phase field used to derive *N*, and rethink how one should use that information in the context of complex terrain.

4.1 Starting to think in 3-D (work in progress)

At its root, the phase φ of a target is a function of the radar frequency *f*, the range of the target *r*, and the refractive index of air *n* averaged over the path length:

$$\varphi = \frac{4\pi f r}{c} n .$$

If we knew the range to each target to sub-mm accuracy, we could use that formula directly to obtain *n*. Instead, we use the change in the phase between two times to obtain the changes in *n* between two times. Assuming *f* and *r* to be constants between these two times t_0 and t_1, we get

$$\Delta\varphi = \varphi(t_1) - \varphi(t_0) = \frac{4\pi f r}{c}\left(n(t_1) - n(t_0)\right) = \frac{4\pi f r}{c}\Delta n .$$

This gives us path-integrated changes in *n*, provided we can dealias properly the measured changes in phase. The technique used until now is based on that equation. But that equation is already misleading, because the path taken by radar waves to go from the radar to the target may have changed between the two times as a result of differences in the vertical gradient of *n*. Already here, the height of the target and along the trajectory must be taken into account.

Let us suppose we want to measure *n* at the surface (since we will use surface data for calibration) and that d*n*/d*h* is constant in height. If h_r and h_i are the altitudes of the radar and of target i above our surface reference height respectively, the height *h(r)* sampled by the beam is

$$h(r) = h_r + \frac{h_i - h_r}{r_i} + \frac{1 + a\dfrac{dn}{dh}}{2a}\left(r^2 - r_i r\right),$$

where *a* is the radius of the Earth. Based on that, the first equation can be rewritten as:

$$\varphi_i = \frac{4\pi f}{c}\int_0^{r_i}\left(n(r) + \frac{dn}{dh}h(r)\right)dr$$

$$= \frac{4\pi f}{c}\left\{\int_0^{r_i} n(r)dr + \frac{dn}{dh}\left[\left(\frac{h_r + h_i}{2}\right)r_i - \frac{1 + a\dfrac{dn}{dh}}{12a}r_i^3\right]\right\}.$$

When we subtract φ_i to the value at the reference time, $\Delta\varphi_i$ becomes

$$\Delta\varphi_i = \frac{4\pi f}{c}\int_0^{r_i}\Delta n(r)\,dr$$
$$+ \frac{4\pi f}{c}\left\{\Delta\left(\frac{dn}{dh}\right)\left[\left(\frac{h_r + h_i}{2}\right)r_i - \frac{r_i^3}{12a}\right] + \Delta\left[\left(\frac{dn}{dh}\right)^2\right]\frac{r_i^3}{12}\right\}.$$

Finally, to get changes in *n* between two neighboring points at ranges r_1 and r_2 along the same azimuth, we must use the information from two targets. Then, the ugly truth becomes:

$$\Delta\varphi(r_2) - \Delta\varphi(r_1) = \frac{4\pi f}{c}\left\{\int_{r_1}^{r_2}\Delta n(r)\,dr + \Delta\left[\left(\frac{dn}{dh}\right)^2\right]\frac{r_2^3 - r_1^3}{12}\right\}$$
$$+ \frac{4\pi f}{c}\Delta\left(\frac{dn}{dh}\right)\left[\frac{h_r(r_2 - r_1) + h_2 r_2 - h_1 r_1}{2} - \frac{r_2^3 - r_1^3}{12a}\right].$$

Therefore, in addition to the wanted quantity (first term), we have additional terms that, to the present technique, just looks like "noise" in the phase data.

Figure 11 shows how each of these terms vary with range for reasonable values for each quantity. One can see that, even at S-band, the magnitude of the "noise" terms can be quite large for modest changes in the height of targets or in the vertical gradient of refractive index.

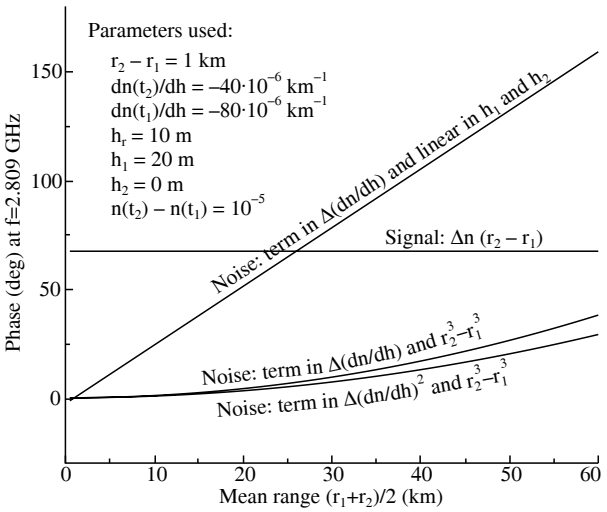

FIG. 11. Magnitude of each of the four major term of the last equation as a function of range.

4.2 Improving phase data quality

In parallel, the range of each target is only known to within a range gate (typically 150 m). That uncertainty adds another small "noise" term proportional to Δ*n* and the uncertainty in range Δ*r*. Finally, as d*n*/d*h* changes, portions of targets that were hidden may become uncovered, and that will also change the phase of the target.

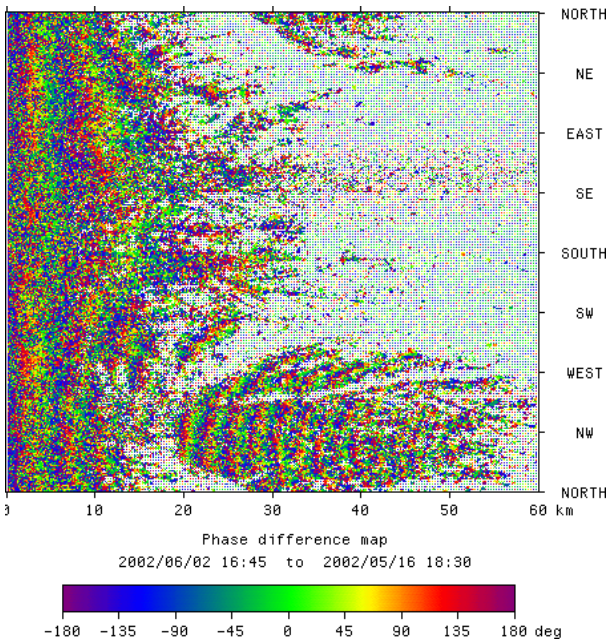

FIG. 12. Raw phase difference of ground targets between two times two weeks apart as measured by S-Pol (f = 2.809 GHz) and displayed in a range-azimuth (B-scan) projection. Note the noisiness of the phase field (this is actually a benign case), and how it increases with range.

When all these "noises" combine, if we look at how *Δφ* changes with range, we do not get a smooth field that aliases like crazy but instead a very noisy field that aliases like crazy (Fig. 12).

In the past, I have stressed the dealiasing of the phase field as a major issue. Phase aliasing surely looks spectacular, but it is not the most crucial issue: if the phase data were highly coherent, dealiasing them would be easy. It is the combination of the space-varying aliasing rate with a phase noise that may exceed 360° at S-band and a lot more at other wavelengths that makes the process challenging. And of course, the most interesting meteorological conditions are the ones that will have the highest *n* and d*n*/d*h* variability; this is why the data quality under these circumstances tend to be the poorest. Note, for example, how the derived *N* field during the outflow case (Fig. 9) have holes or suspicious values along some radials.

Except for the "noise" caused by the apparent changing shape of targets, all of the other terms are predictable. The trick would be to somehow obtain information on target height and on d*n*/d*h* to be able to compensate for these effects. While a statistical approach such as smoothing may help diminish the problem, I believe that the predictable sources of errors should be fixed intelligently; we should only use statistical or other "brute force" approach when we are out of options. We have learned (are still learning?) the hard way that to get good rainfall data from radar, we must first clean the data, remove all known artifacts, correct for known errors, before we can use brute force approaches such as raingauge calibration to get good results. It will require ingenuity, but let us try not to repeat the same mistake for refractivity.

5. REFERENCES

Crook, N.A., and J.B. Klemp, 2000: Lifting by convergence lines. *J. Atmos. Sci.*, **57**, 873-890.

Demoz, B., et al., 2005: The dryline on 22 May 2002 during IHOP_2002: convective scale measurements at the profiling site. *Mon. Wea. Rev.*, **133**, IHOP issue.

Fabry, F., C. Frush, A. Kilambi, and I. Zawadzki, 1997: On the extraction of near-surface index of refraction using radar measurements of ground targets. *J. Atmos. Oceanic Technol.*, **14**, 978-987.

Fabry, F., 2004: Meteorological value of ground target measurements by radar. *J. Atmos. Oceanic Technol.*, **21**, 560-573.

Fabry, F., 2005: The spatial variability of moisture in the boundary layer and its effect on convection initiation: project-long characterization. *Mon. Wea. Rev.*, **133**, IHOP issue.

Weckwerth, T.M., et al., 2004: An overview of the International H_2O Project (IHOP_2002) and some preliminary highlights. *Bull. Amer. Meteorol. Soc.*, **85**, 253-277.

Weckwerth, T.M., C.R. Pettet, F. Fabry, S. Park, J.W. Wilson, and M.A. LeMone, 2005: Radar refractivity retrieval: Validation and application to short-term forecasting. *J. Applied Meteor.*, **44**, 285-300.